Vietnam Journal of Mechanics, VAST, Vol. 40, No. 2 (2018), pp. 141 – 154
DOI:10.15625/0866-7136/10564

ROBUST CONTROL FOR A WHEELED MOBILE ROBOT TO TRACK A PREDEFINED TRAJECTORY IN THE PRESENCE OF UNKNOWN WHEEL SLIPS

Kiem Nguyentien[1], Linh Le[2], Tuan Do[3], Tinh Nguyen[3,*], Minhtuan Pham[4]
[1]*Hanoi University of Industry, Hanoi, Vietnam*
[2]*University of Information and Communication Technology, Thai Nguyen University, Vietnam*
[3]*Institute of Information Technology, VAST, Hanoi, Vietnam*
[4]*Space Technology Institute, VAST, Hanoi, Vietnam*
[*]E-mail: nvtinh@ioit.ac.vn
Received July 21, 2017

Abstract. In this paper, a robust controller for a nonholonomic wheeled mobile robot (WMR) is proposed for tracking a predefined trajectory in the presence of unknown wheel slips, bounded external disturbances, and model uncertainties. The whole control system consists of two closed loops. Specifically, the outer one is employed to control the kinematics, and the inner one is used to control the dynamics. The output of kinematic controller is adopted as the input of the inner (dynamic) closed loop. Furthermore, two robust techniques were utilized to assure the robustness. In particular, one is used in the kinematic controller to compensate the harmful effects of the unknown wheel slips, and the other is used in the dynamic controller to overcome the model uncertainties and bounded external disturbances. Thanks to this proposed controller, a desired tracking performance in which tracking errors converge asymptotically to zero is obtained. According to Lyapunov theory and LaSalle extension, the desired tracking performance is guaranteed to be achieved. The results of computer simulation have shown the validity and efficiency of the proposed controller.

Keywords: Asymptotic convergence to zero, bounded external disturbances, desired tracking performance, model uncertainties, unknown wheel slips.

1. INTRODUCTION

It is well known that wheeled mobile robots are able to work effectively in a wide area, and especially they are capable of performing tasks intelligently without any human action. In addition, they can replace people on dangerous tasks such as looking for explosive materials, transporting of goods in environments having poison, rescue, etc., and therefore they have had wide applicability and been increasingly popular in various areas such as industry, entertainment, healthcare, automation in logistics, transport, etc.

Furthermore, a WMR is one of the systems suffering nonholonomic constraints, and therefore researchers all over the world have paid much their attention to study this topic Recently, a lot of the effort of researchers in the world has been paid in order to solve the tracking control problems of WMRs by employing various control techniques such as sliding mode control [1], adaptive control [2], backstepping control [3, 4], etc. Most previous works have been performed under an assumption that "pure rolling without slip" has held.

Conversely, unfortunately, in a number of practical applications, such the assumption has usually been violated. There simply existed wheel slips. Clearly, the wheel slip has been one of the reasons making tracking performance of a WMR be worse significantly. Accordingly, a robust tracking controller must be proposed in such a way that it is capable of compensating the effects of the wheel slips to achieve a desired tracking performance.

To be specific, with the aim of addressing the undesired influences of the wheel slips, an adaptive tracking controller was derived in [5], which is based on slip-ratios. Methods based on gyros and accelerometers to cope with the wheel slips in the realtime were also shown in [6, 7]. The authors in [8] proposed a feedback linearization controller for tracking a desired trajectory of a WMR in the presence of the longitudinal and lateral slip at each driving wheel under an ideal condition where model uncertainties and unknown bounded external disturbances were ignored, and furthermore the values of the accelerations and velocities of the wheel slips could be accurately measured Nevertheless, it is impractical to obtain an acceptable performance by adopting this feedback linearization controller in real applications. The reason is that such an ideal condition is unrealistic and therefore does not exist in practice In [9], a tracking control problem was addressed in the world coordinate system by means of a neural network-based adaptive tracking controller being capable of compensating the effects the wheel slips, where the neural network weight updating law was built by making an objective function minimal. In [10], an adaptive controller based on a nonlinear disturbance observer was proposed at the dynamic level and in the polar coordinate system for trajectory tracking of a class of Type (2, 0) WMRs.

Overall, most these works were fulfilled under a condition that the accelerations and velocities of the wheel slips have been measured exactly for analyzing and designing controllers being robust against the wheel slips. The drawback of this condition is the extra requirement of expensive and complex sensors so as to measure the wheel slips such as a global position system (GPS), a gyroscope, an accelerometer, etc.

These results have motivated us to propose a robust tracking control method based on the backstepping technique [3] for a WMR with the unknown wheel slips, model uncertainties, and unknown bounded external disturbances in such a way that the WMR tracks a predefined trajectory with a desired tracking performance where the convergence to zero of the tracking errors is ensured Furthermore, this proposed control method has relaxed the measurements of the accelerations and velocities of the wheel slips. The entire control system includes two closed loops. To be specific, the outer one is adopted in order to control the kinematics, and the other is used to control the dynamics Moreover, two robust techniques were utilized to assure the robustness. In particular, one is used

in the kinematic controller so as to overcome the harmful effects of the unknown wheel slips, and the other is used in the dynamic controller to deal with the model uncertainties and bounded external disturbances.

The structure of this article is organized as follows. Section 2 shows preliminaries namely the kinematics and dynamics of the WMR with the wheel slips. Section 3 expresses a procedure designing the proposed control law. Section 4 illustrates comparative computer simulation results carried out via Matlab/Simulink software. Finally, Section 5 describes our conclusions.

2. PRELIMINARIES

2.1. The kinematics of the WMR with the wheel slips

Let us consider a nonholonomic WMR composed of two driving wheels and a caster wheel as shown in Fig. 1. Specifically, G with coordinates (x_G, y_G) is the center of mass of the platform of the WMR. M with coordinates (x_M, y_M) indicates the midpoint of the wheel shaft. F_1 and F_2 illustrate the total longitudinal friction forces at the right and left driving wheel, respectively. F_3 expresses the total lateral friction force along the wheel shaft. F_4 and ϖ describe external force and moment acting on G, respectively. r is the radius of each driving wheel. b shows the haft of the wheel shaft. θ is the angle showing the orientation of the WMR.

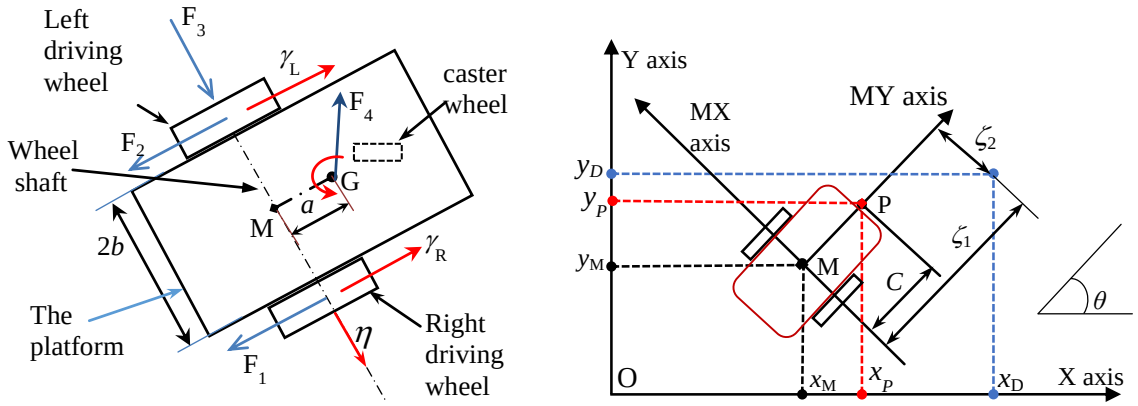

Fig. 1. (a) A nonholonomic WMR subjected to unknown wheel slips; (b) The coordinate of the target is represented in the body coordinate system M-XY

Without the wheel slips, the linear and angular velocities of the WMR, calculated at M, are expressed respectively as follows [3]

$$\Theta = \frac{r\left(\dot{\phi}_R + \dot{\phi}_L\right)}{2}, \quad \mu = \frac{r\left(\dot{\phi}_R - \dot{\phi}_L\right)}{2b}, \tag{1}$$

where $\dot{\phi}_R, \dot{\phi}_L$ denote the angular velocities of the right and left driving wheel about the wheel shaft, respectively.

Thus, the kinematics of the WMR is shown as follows [3]

$$\begin{cases} \dot{x}_M = \Theta \cos\theta, \\ \dot{y}_M = \Theta \sin\theta, \\ \mu = \dot{\theta}. \end{cases} \tag{2}$$

On the other hand, if the WMR moves in the presence of the wheel slips, then (1) and (2) do not hold. Now, let us denote γ_R and γ_L as the coordinate of the longitudinal slip of the right and left driving wheels, respectively, and η as the coordinate of the lateral slip along the wheel shaft (see Fig. 1), with the result that the actual linear velocity of the WMR along the longitudinal direction is described as follows [8]

$$\vartheta = \frac{r\left(\dot{\phi}_R + \dot{\phi}_L\right)}{2} + \frac{\dot{\gamma}_R + \dot{\gamma}_L}{2} = \Theta + \frac{\dot{\gamma}_R + \dot{\gamma}_L}{2}. \tag{3}$$

The actual angular velocity of the WMR is computed as follows [8]

$$\omega = \frac{r\left(\dot{\phi}_R - \dot{\phi}_L\right)}{2b} + \frac{\dot{\gamma}_R - \dot{\gamma}_L}{2b} = \mu + \frac{\dot{\gamma}_R - \dot{\gamma}_L}{2b}. \tag{4}$$

Thus, the kinematic model of this WMR can be expressed as follows [8]

$$\begin{cases} \dot{x}_M = \vartheta \cos\theta - \dot{\eta} \sin\theta, \\ \dot{y}_M = \vartheta \sin\theta + \dot{\eta} \cos\theta, \\ \dot{\theta} = \omega. \end{cases} \tag{5}$$

The perturbed nonholonomic constrains can in turn be written as follows [10]

$$\begin{cases} \dot{\gamma}_R = -r\dot{\phi}_R + \dot{x}_M \cos\theta + \dot{y}_M \sin\theta + b\omega, \\ \dot{\gamma}_L = -r\dot{\phi}_L + \dot{x}_M \cos\theta + \dot{y}_M \sin\theta - b\omega, \\ \dot{\eta} = -\dot{x}_M \sin\theta + \dot{y}_M \cos\theta. \end{cases} \tag{6}$$

2.2. Dynamics of the WMR with wheel slips

Let $\mathbf{q} = [x_G, y_G, \theta, \eta, \gamma_R, \gamma_L, \phi_R, \phi_L]^T$ be a vector of generalized Lagrange coordinates. The perturbed nonholonomic constrains (6) can be expressed in term of matrix as follows

$$\mathbf{A}(\mathbf{q})\,\dot{\mathbf{q}} = \mathbf{0}. \tag{7}$$

with $\mathbf{A}(\mathbf{q}) = \begin{bmatrix} \cos\theta & \sin\theta & b & 0 & -1 & 0 & -r & 0 \\ \cos\theta & \sin\theta & -b & 0 & 0 & -1 & 0 & -r \\ -\sin\theta & \cos\theta & a & -1 & 0 & 0 & 0 & 0 \end{bmatrix}$, where a is the distance between M and G (see Fig. 1).

According to Euler–Lagrange formulation, the dynamic model of this WMR is shown as follows [3]

$$\overline{\mathbf{M}}(\mathbf{q})\,\ddot{\mathbf{q}} + \overline{\boldsymbol{\tau}}_d = \mathbf{N}\boldsymbol{\tau} + \mathbf{A}^T(\mathbf{q})\,\boldsymbol{\lambda}, \tag{8}$$

where $\boldsymbol{\lambda} = [\lambda_1, \lambda_2, \lambda_3]^T$ is the vector of Lagrange multipliers to be considered as nonholonomic constraint factors. $\boldsymbol{\tau} = [\tau_R, \tau_L]^T$ is the input vector with τ_R and τ_L showing the torques at the right and left driving wheel about the wheel shaft, respectively. $\overline{\boldsymbol{\tau}}_d$ is a vector describing both the model uncertainties such as unstructured unmodelled dynamic components and the unknown bounded external disturbances for example unknown external forces as F_1, F_2, F_3, F_4, ϖ (see Fig. 1(a)).

$\mathbf{N} = \begin{bmatrix} 0 & 0 & 0 & 0 & 0 & 0 & 1 & 0 \\ 0 & 0 & 0 & 0 & 0 & 0 & 0 & 1 \end{bmatrix}^T$ is the input transformation matrix.

Replacing (x_M, y_M) in (5) and (6) by (x_G, y_G), it is possible to show that

$$\dot{\mathbf{q}} = \mathbf{S}_1(\mathbf{q})\,\mathbf{v} + \mathbf{S}_2(\mathbf{q})\,\dot{\boldsymbol{\gamma}} + \mathbf{S}_3(\mathbf{q})\,\dot{\boldsymbol{\eta}}, \tag{9}$$

where $\mathbf{v} = [\dot{\phi}_R, \dot{\phi}_L]^T$, $\boldsymbol{\gamma} = [\gamma_R, \gamma_L]^T$. Here, $\mathbf{S}_1(\mathbf{q})$, $\mathbf{S}_2(\mathbf{q})$ and $\mathbf{S}_3(\mathbf{q})$ are possibly given by

$$\mathbf{S}_1 = \begin{bmatrix} \left(\frac{r}{2}\cos\theta - \frac{ar}{2b}\sin\theta\right) & \left(\frac{r}{2}\sin\theta + \frac{ar}{2b}\cos\theta\right) & \frac{r}{2b} & 0 & 0 & 0 & 1 & 0 \\ \left(\frac{r}{2}\cos\theta + \frac{ar}{2b}\sin\theta\right) & \left(\frac{r}{2}\sin\theta - \frac{ar}{2b}\cos\theta\right) & -\frac{r}{2b} & 0 & 0 & 0 & 0 & 1 \end{bmatrix}^T,$$

$$\mathbf{S}_2 = \begin{bmatrix} \left(\frac{1}{2}\cos\theta - \frac{a}{2b}\sin\theta\right) & \left(\frac{1}{2}\sin\theta + \frac{a}{2b}\cos\theta\right) & \frac{1}{2b} & 0 & 1 & 0 & 0 & 0 \\ \left(\frac{1}{2}\cos\theta + \frac{a}{2b}\sin\theta\right) & \left(\frac{1}{2}\sin\theta - \frac{a}{2b}\cos\theta\right) & -\frac{1}{2b} & 0 & 0 & 1 & 0 & 0 \end{bmatrix}^T,$$

$$\mathbf{S}_3 = \begin{bmatrix} -\sin\theta & \cos\theta & 0 & 1 & 0 & 0 & 0 & 0 \end{bmatrix}^T.$$

Subsequently, taking the time derivative of (9), we obtain

$$\ddot{\mathbf{q}} = \dot{\mathbf{S}}_1(\mathbf{q})\,\mathbf{v} + \mathbf{S}_1(\mathbf{q})\,\dot{\mathbf{v}} + \mathbf{S}_2(\mathbf{q})\,\ddot{\boldsymbol{\gamma}} + \dot{\mathbf{S}}_2(\mathbf{q})\,\dot{\boldsymbol{\gamma}} + \dot{\mathbf{S}}_3(\mathbf{q})\,\dot{\boldsymbol{\eta}} + \mathbf{S}_3(\mathbf{q})\,\ddot{\boldsymbol{\eta}}. \tag{10}$$

On the other hand, one can easily see that

$$\mathbf{A}(\mathbf{q})\,\mathbf{S}_1(\mathbf{q}) = \mathbf{0} \quad \text{and} \quad \mathbf{S}_1^T(\mathbf{q})\,\mathbf{N} = \mathbf{I}. \tag{11}$$

Substituting (10) into (8), and then pre-multiplying the both sides of the new equation by $\mathbf{S}_1^T(\mathbf{q})$, it results in

$$\mathbf{M}\dot{\mathbf{v}} + \mathbf{B}(\mathbf{v})\,\mathbf{v} + \boldsymbol{\Omega}\mathbf{v} + \mathbf{Q}\ddot{\boldsymbol{\gamma}} + \mathbf{C}\dot{\boldsymbol{\eta}} + \mathbf{G}\ddot{\boldsymbol{\eta}} + \boldsymbol{\tau}_d = \boldsymbol{\tau}, \tag{12}$$

where $\boldsymbol{\tau}_d = \mathbf{S}_1^T(\mathbf{q})\,\overline{\boldsymbol{\tau}}_d$. The matrices in (12) are shown specifically as follows

$$\mathbf{M} = \mathbf{S}_1^T\overline{\mathbf{M}}\mathbf{S}_1 = \begin{bmatrix} m_{11} & m_{12} \\ m_{12} & m_{11} \end{bmatrix}, \quad \mathbf{Q} = \mathbf{S}_1^T\overline{\mathbf{M}}\mathbf{S}_2 = \begin{bmatrix} Q_1 & Q_2 \\ Q_2 & Q_1 \end{bmatrix},$$

$$\mathbf{C} = \mathbf{S}_1^T\mathbf{M}\dot{\mathbf{S}}_3 = m_G\frac{r}{2}\begin{bmatrix} 1 \\ 1 \end{bmatrix}\omega, \quad \mathbf{G} = \mathbf{S}_1^T\mathbf{M}\mathbf{S}_3 = m_G\frac{ar}{2b}\begin{bmatrix} 1 \\ -1 \end{bmatrix},$$

$$m_{12} = m_G\left(\frac{r^2}{4} - \frac{a^2r^2}{4b^2}\right) - \frac{r^2}{4b^2}\left(I_G + 2I_D\right),$$

$$m_{11} = m_G\left(\frac{r^2}{4} + \frac{a^2r^2}{4b^2}\right) + \frac{r^2}{4b^2}\left(I_G + 2I_D\right) + m_W r^2 + I_W,$$

$$Q_{1,2} = m_G\frac{r}{4}\left(1 \pm \frac{a^2}{b^2}\right) \pm \frac{r}{4b}\left(I_G + 2I_D\right),$$

$$\boldsymbol{\Omega} = m_G\frac{ar^2}{2b}\frac{\dot{\gamma}_R - \dot{\gamma}_L}{2b}\begin{bmatrix} 0 & 1 \\ -1 & 0 \end{bmatrix},$$

$$\mathbf{B}(\mathbf{v}) = m_G\frac{ar^2}{2b}\mu\begin{bmatrix} 0 & 1 \\ -1 & 0 \end{bmatrix} = m_G\frac{ar^2}{2b}\frac{r\left(\dot{\phi}_R - \dot{\phi}_L\right)}{2b}\begin{bmatrix} 0 & 1 \\ -1 & 0 \end{bmatrix}.$$

The parameters of the WMR in the above matrices are described in Tab. 1.

Table 1. The parameters of the WMR [3]

Symbol	Quantity	Value
m_G	The mass of the platform of the WMR	10 (kg)
I_G	The inertial moment of the platform about the vertical axis through G	5 (kg.m^2)
a	The distance between G and M (see Fig. 1(a))	0.2 (m)
C	The distance between P and M (see Fig. 1(b))	0.5 (m)
m_W	The mass of each driving wheel	2 (kg)
I_W	The inertial moment of each driving wheel about the wheel shaft	0.1 (kg.m^2)
I_D	The inertial moment of each wheel about its diameter axis	0.05 (kg.m^2)
b	half-distance between two the driving wheels	0.25 (m)
r	The radius of each driving wheel	0.05 (m)

We have 2 following properties.

Property 1. $\mathbf{M}$ is always an invertible, differentiable, and positive-definite.

Property 2. $\left[\dot{\mathbf{M}} - 2\mathbf{B}\left(\mathbf{v}\right)\right]$ is a skew-symmetric matrix. In other words, it implies that $\mathbf{x}^T \left[\dot{\mathbf{M}} - 2\mathbf{B}\left(\mathbf{v}\right)\right] \mathbf{x} = 0$ with $\forall \mathbf{x} \in \mathbf{R}^{2\times 1}$.

3. DESIGNING CONTROL LAW

3.1. Problem statement

The control goal is to design an adaptive tracking controller for the WMR subjected to the unknown wheel slips, the model uncertainties, and the unknown bounded external disturbances in such a way that the point P of the WMR (see Fig. 1) seems to track the target D with a predefined tracking performance in the absence of measuring the accelerations and velocities of the wheel slips. For this purpose, we have proposed the scheme of the whole control system as shown in Fig. 2.

Remark 1. From Fig. 1, let (x_P, y_P, θ) and $(x_{Pd}, y_{Pd}, \theta_d)$ be the actual and desired posture of the WMR, respectively. It is infeasible to obtain an arbitrarily good tracking performance in a finite-time interval if one wants to control the WMR in such a way that the actual posture (x_P, y_P, θ) tracks the desired one $(x_{Pd}, y_{Pd}, \theta_d)$ successfully in the presence of the wheel slips, namely both longitudinal slips and lateral slip between the driving wheels and the floor. On the other hand, an arbitrarily good tracking performance in a finite-time interval is fully achievable if one wants to control the WMR with the purpose of making the actual position (x_P, y_P) track the desired one (x_{Pd}, y_{Pd}) in such situations (see Definition 1 and Definition 2 in [11]).

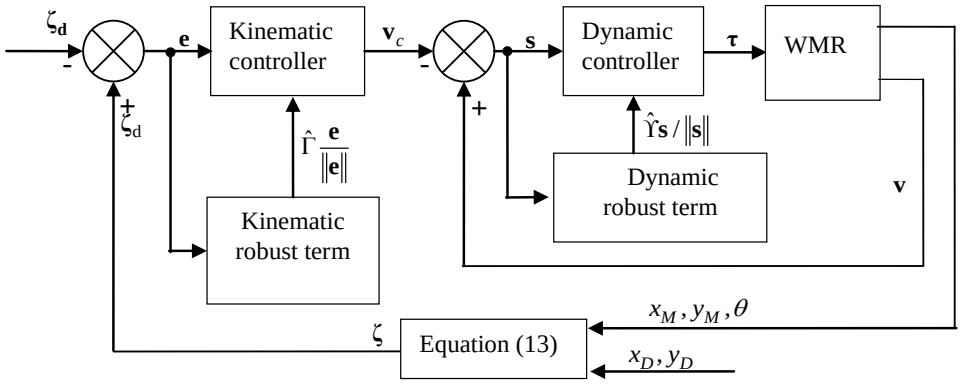

Fig. 2. Scheme of the whole closed-loop control system

3.2. Robust kinematic control law

Firstly, let O-XY denote the global coordinate system and M-XY denote the body coordinate system attached to the WMR's platform (see Fig. 1(b)). The coordinate vector of the target D is expressed in M-XY as follows

$$\boldsymbol{\zeta} = \begin{bmatrix} \zeta_1 \\ \zeta_2 \end{bmatrix} = \begin{bmatrix} \cos\theta & \sin\theta \\ -\sin\theta & \cos\theta \end{bmatrix} \begin{bmatrix} x_D - x_M \\ y_D - y_M \end{bmatrix}, \tag{13}$$

where (x_D, y_D) is the Cartesian coordinate of D in O-XY (see Fig. 1(b)).

Taking the first order derivative with respect to time of (13) yields

$$\mathbf{i} = \mathbf{h}\mathbf{v} + \begin{bmatrix} \cos\theta & \sin\theta \\ -\sin\theta & \cos\theta \end{bmatrix} \begin{bmatrix} \dot{x}_D \\ \dot{y}_D \end{bmatrix} + \boldsymbol{\chi}, \tag{14}$$

where $\mathbf{h} = \begin{bmatrix} \left(\zeta_2 \frac{1}{b} - 1\right)\frac{r}{2} & -\left(\zeta_2 \frac{1}{b} + 1\right)\frac{r}{2} \\ -\zeta_1 \frac{r}{2b} & \zeta_1 \frac{r}{2b} \end{bmatrix}, \boldsymbol{\chi} = \begin{bmatrix} -\frac{\dot{\gamma}_R + \dot{\gamma}_L}{2} \\ -\dot{\eta} \end{bmatrix}.$

Remark 2. Because of $\det(\mathbf{h}) = -\zeta_1 \frac{r^2}{2b}$, it follows that $\mathbf{h}$ is invertible as long as $\zeta_1 \neq 0$.

Assumption 1. Not only x_D, y_D but also their first and second derivatives are bounded.

Assumption 2. All $\dot{\gamma}_R, \dot{\gamma}_L$ and $\dot{\eta}$ are bounded. Therefore, there exists an unknown positive constant value Γ such that $\|\boldsymbol{\chi}\| \leq \Gamma$.

From the control goal stated in Subsection 3.1 and Fig. 1, it is possible to express the desire vector of $\boldsymbol{\zeta}$ as $\boldsymbol{\zeta}_d = [C, 0]^T$, and therefore the vector of the position tracking errors is calculated as $\mathbf{e} = [e_1, e_2]^T = \boldsymbol{\zeta} - \boldsymbol{\zeta}_d$.

As the velocities of the wheel slips are not measured, $\boldsymbol{\chi}$ in (14) is unknown. Consequently, let us propose a desired vector of the wheel angular velocity $\mathbf{v}$ as follows

$$\mathbf{v}_c = \mathbf{h}^{-1}\left(-\boldsymbol{\Lambda}\mathbf{e} + \mathbf{i}_d - \begin{bmatrix} \cos\theta & \sin\theta \\ -\sin\theta & \cos\theta \end{bmatrix} \begin{bmatrix} \dot{x}_D \\ \dot{y}_D \end{bmatrix} - \hat{\boldsymbol{\chi}}\right), \tag{15}$$

where $\widehat{\boldsymbol{\chi}}$ is the kinematic robust term which eliminates the harmful effects of the wheel slips at the kinematic level to establish the robustness of the kinematic closed control loop (see Fig. 2), and $\boldsymbol{\Lambda}$ is a positive definite matrix and can be selected arbitrarily.

Replacing $\mathbf{v}$ in (14) by $\mathbf{v}_c$ in (15) yields

$$\dot{\mathbf{e}} = -\boldsymbol{\Lambda}\mathbf{e} + \boldsymbol{\chi} - \widehat{\boldsymbol{\chi}}. \tag{16}$$

Let us propose the kinematic robust term as follows

$$\widehat{\boldsymbol{\chi}} = \widehat{\Gamma}\frac{\mathbf{e}}{\|\mathbf{e}\|} \quad \text{with} \quad \dot{\widehat{\Gamma}} = \mathrm{H}\,\|\mathbf{e}\|\,, \tag{17}$$

where H expresses a positive real constant and can be chosen arbitrarily. $\widehat{\Gamma}$ is the kinematic robust gain and updated online.

3.3. Robust dynamic control law

Adding $-\mathbf{M}\dot{\mathbf{v}}_c - \mathbf{B}(\mathbf{v})\,\mathbf{v}_c$ to the both sides of (12) results in

$$\mathbf{M}\dot{\mathbf{s}} = \boldsymbol{\tau} - \mathbf{B}(\mathbf{v})\,\mathbf{s} - \mathbf{M}\dot{\mathbf{v}}_c - \mathbf{B}(\mathbf{v})\,\mathbf{v}_c + \boldsymbol{\delta}, \tag{18}$$

with $\mathbf{s} = \mathbf{v} - \mathbf{v}_c$ being the velocity tracking error vector, and $\boldsymbol{\delta} = -\boldsymbol{\Omega}\mathrm{v} - \mathbf{Q}\ddot{\boldsymbol{\gamma}} - \mathbf{C}\dot{\boldsymbol{\eta}} - \mathbf{G}\ddot{\boldsymbol{\eta}} - \boldsymbol{\tau}_d$.

It should be noted that there is no prior knowledge of the dynamic parameters of the WMR exactly. Therefore, let us propose the torque input as follows

$$\boldsymbol{\tau} = -\mathbf{K}\mathbf{s} + \widehat{\mathbf{M}}\dot{\mathbf{v}}_c + \widehat{\mathbf{B}}(\mathbf{v})\,\mathbf{v}_c - \widehat{\mathbf{d}}, \tag{19}$$

where $\mathbf{K}$ is a positive-definite diagonal constant matrix and can be chosen arbitrarily. $\widehat{\mathbf{M}}$ and $\widehat{\mathbf{B}}(\mathbf{v})$ are the estimation of $\mathbf{M}$ and $\mathbf{B}(\mathbf{v})$, respectively. $\widehat{\mathbf{d}}$ shows the dynamic robust term to eliminate the total uncertainty owing to the model uncertainties and unknown bounded external disturbances and to be determined subsequently.

Utilizing the control input (19) makes the dynamics of $\mathbf{s}$ in (18) become

$$\mathbf{M}\dot{\mathbf{s}} = -\mathbf{B}(\mathbf{v})\,\mathbf{s} - \mathbf{K}\mathbf{s} + \mathbf{d} - \widehat{\mathbf{d}}, \tag{20}$$

with $\mathbf{d} = \boldsymbol{\delta} - \widetilde{\mathbf{M}}\dot{\mathrm{v}}_c - \widetilde{\mathbf{B}}(\mathbf{v})\,\mathbf{v}_c$, $\widetilde{\mathbf{M}} = \mathbf{M} - \widehat{\mathbf{M}}$, $\widetilde{\mathbf{B}}(\mathbf{v}) = \mathbf{B}(\mathbf{v}) - \widehat{\mathbf{B}}(\mathbf{v})$.

Assumption 3. $\mathbf{d}$ is bounded by an unknown positive value, which implies that $\|\mathbf{d}\| \leq \mathrm{Y}$.

On the other hand, the dynamic robust term $\widehat{\mathbf{d}}$ in (19) is proposed as follows

$$\widehat{\mathbf{d}} = \widehat{\mathrm{Y}}\frac{\mathbf{s}}{\|\mathbf{s}\|} \quad \text{with} \quad \dot{\widehat{\mathrm{Y}}} = \Psi\,\|\mathbf{s}\|\,, \tag{21}$$

with Ψ being positive constants and being selected arbitrarily. $\widehat{\mathrm{Y}}$ is the dynamic robust gain and updated online.

3.4. Stability analysis

Theorem 1. *Let us take account of the WMR in the presence of the unknown wheel slips, model uncertainties, bounded external disturbances with the kinematics (5) and the dynamics (12) under a condition that Assumptions 1–3 hold. If the proposed control method as shown Fig. 2 with the kinematic control law (15) and dynamic control law (19) is utilized, then the tracking error vectors consisting of* $\mathbf{e}$ *and* $\mathbf{s}$ *asymptotically converge to zero as* $t \to \infty$ *and the control parameters are ensured to be bounded for all* $t > 0$.

Proof. Let us choose a candidate Lyapunov function as follows

$$V = \frac{1}{2}\mathbf{e}^T\mathbf{e} + \frac{1}{2}\mathbf{s}^T\mathbf{M}\mathbf{s} + \frac{1}{2}H^{-1}\widetilde{\Gamma}^2 + \frac{1}{2}\Psi^{-1}\widetilde{\Upsilon}^2, \tag{22}$$

with $\widetilde{\Upsilon} = \Upsilon - \widehat{\Upsilon}$, $\widetilde{\Gamma} = \Gamma - \widehat{\Gamma}$.

Taking the first derivative of (22), it follows that

$$\dot{V} = \mathbf{e}^T\dot{\mathbf{e}} + \mathbf{s}^T\mathbf{M}\dot{\mathbf{s}} + \frac{1}{2}\mathbf{s}^T\dot{\mathbf{M}}\mathbf{s} - H^{-1}\widetilde{\Gamma}\dot{\widehat{\Gamma}} - \Psi^{-1}\widetilde{\Upsilon}\dot{\widehat{\Upsilon}}. \tag{23}$$

Putting (16), (17), (20), and (21) into (23) with noting Property 2 leads to

$$\dot{V} = -\mathbf{e}^T\mathbf{\Lambda}\mathbf{e} + \mathbf{e}^T\boldsymbol{\chi} - \widehat{\Gamma}\|\mathbf{e}\| - \widetilde{\Gamma}\|\mathbf{e}\| + \mathbf{s}^T\mathbf{d} - \widetilde{\Upsilon}\|\mathbf{s}\| - \widehat{\Upsilon}\|\mathbf{s}\| - \mathbf{s}^T\mathbf{K}\mathbf{s}. \tag{24}$$

According to Assumptions 2–3, it implies that

$$\dot{V} \leq -\mathbf{e}^T\mathbf{\Lambda}\mathbf{e} - \mathbf{s}^T\mathbf{K}\mathbf{s}. \tag{25}$$

For this reason, it follows that $\dot{V} \leq 0$ with $\forall \mathbf{s}, \mathbf{e}$. Applying Lyapunov theory and LaSalle extension, thus allowing for $V(t) \leq V(0)$, has resulted in that if $\mathbf{s}$, $\mathbf{e}$, $\widetilde{\Gamma}$, and $\widetilde{\Upsilon}$ were bounded at the initial time $t = 0$, then they all also will be ensured to be bounded for all $t > 0$. As a consequence of this, all $\mathbf{v}_c, \boldsymbol{\zeta}$, $\widehat{\Gamma}$, and $\widehat{\Upsilon}$ are bounded for all $t > 0$.

In order to apply Barbalat's lemma [12], we define another candidate Lyapunov function as follows

$$V_2 = V - \int_0^t \left[\dot{V}(\iota) + \mathbf{e}^T(\iota)\mathbf{\Lambda}\mathbf{e}(\iota) + \mathbf{s}^T(\iota)\mathbf{K}\mathbf{s}(\iota)\right] d\iota. \tag{26}$$

Differentiating (26) yields

$$\dot{V}_2 = -\mathbf{e}^T\mathbf{\Lambda}\mathbf{e} - \mathbf{s}^T\mathbf{K}\mathbf{s}. \tag{27}$$

Now let us check the uniform continuity of $\dot{V}_2$ whose first derivative is computed as follows

$$\ddot{V}_2 = -2\mathbf{e}^T\mathbf{\Lambda}\dot{\mathbf{e}} - 2\mathbf{s}^T\mathbf{K}\dot{\mathbf{s}}. \tag{28}$$

Every term in (16) as well as (20) is bounded, thus allowing for that $\ddot{V}$ is guaranteed to be bounded, which in turn leads to that $\dot{V}_2$ is uniformly continuous. In accordance with Barbalat's lemma, we can conclude that $\dot{V}_2 \to 0$ as $t \to \infty$, which causes that not only $\mathbf{e}$ but also $\mathbf{s}$ asymptotically converge to zero.

Remark 3. In order to remove the chattering in the output of the kinematic controller, $\mathbf{v}_c$, let us replace (17) by the following equation.

$$\widehat{\boldsymbol{\chi}} = \begin{cases} \widehat{\Gamma}\dfrac{\mathbf{e}}{\|\mathbf{e}\|} & \text{if} \quad \|\mathbf{e}\| > \varsigma \\ \widehat{\Gamma}\dfrac{\mathbf{e}}{\varsigma} & \text{if} \quad \|\mathbf{e}\| \leq \varsigma \end{cases} \quad \text{with} \quad \dot{\widehat{\Gamma}} = \begin{cases} \mathrm{H}\|\mathbf{e}\| & \text{if} \quad \|\mathbf{e}\| > \varsigma \\ 0 & \text{if} \quad \|\mathbf{e}\| \leq \varsigma \end{cases} \tag{29}$$

where ς is a tiny positive real constant value illustrating a boundary layer around zero and can be chosen arbitrarily.

Let us check the stability of the kinematic control closed loop whenever $\|\mathbf{e}\| \leq \varsigma$ by selecting another candidate Lyapunov function as follows

$$V_3 = \frac{1}{2}\mathbf{e}^T\mathbf{e}. \tag{30}$$

Taking the time derivative of (30) results in

$$\dot{V}_3 = \mathbf{e}^T\dot{\mathbf{e}}. \tag{31}$$

Substitution (16) and (29) in case $\|\mathbf{e}\| \leq \varsigma$ into (31) yields

$$\dot{V}_3 = -\mathbf{e}^T\left(\mathbf{\Lambda}\mathrm{e} - \boldsymbol{\chi} + \frac{\widehat{\Gamma}}{\varsigma}\mathbf{e}\right). \tag{32}$$

Applying Assumption 2 shows that

$$\dot{V}_3 \leq -\|\mathbf{e}\|\left[\left(\Lambda_{\min} + \frac{\widehat{\Gamma}}{\varsigma}\right)\|\mathbf{e}\| - \Gamma\right], \tag{33}$$

where $\Lambda_{\min}$ is the minimum eigenvalue of $\mathbf{\Lambda}$.

Seeing (33) describes that $\dot{V}_3$ is assured to be negative as long as the term in the braces is strictly positive. Particularly, $\dot{V}_3$ is negative if the following inequality holds.

$$\left(\Lambda_{\min} + \frac{\widehat{\Gamma}}{\varsigma}\right)\|\mathbf{e}\| > \Gamma. \tag{34}$$

As a result, according to Lyapunov criteria and LaSalle extension, it can be easily shown that $\mathbf{e}$ is guaranteed to be uniformly ultimately bounded in the following compact set.

$$\mathbf{U_e} = \left\{\mathbf{e} \in \mathbf{R}^{2\times 1}\,\middle|\,\left(\Lambda_{\min} + \frac{\widehat{\Gamma}}{\varsigma}\right)\|\mathbf{e}\| \leq \Gamma\right\}. \tag{35}$$

Moreover, it is clear that $\mathbf{e}$ can be kept arbitrarily small by choosing $\mathbf{\Lambda}$ to be proper. Particularly, the bigger $\Lambda_{\min}$ is, the smaller $\mathbf{e}$ is.

Remark 4. In order to alleviate the chattering at the dynamic level, (21) is proposed to be replaced by the following equations.

$$\widehat{\mathbf{d}} = \begin{cases} \widehat{\Upsilon}\dfrac{\mathbf{s}}{\|\mathbf{s}\|} & \text{if} \quad \|\mathbf{s}\| > \kappa \\ \widehat{\Upsilon}\dfrac{\mathbf{s}}{\kappa} & \text{if} \quad \|\mathbf{s}\| \leq \kappa \end{cases} \quad \text{with} \quad \dot{\widehat{\Upsilon}} = \begin{cases} \Psi\|\mathbf{s}\| & \text{if} \quad \|\mathbf{s}\| > \kappa \\ 0 & \text{if} \quad \|\mathbf{s}\| \leq \kappa \end{cases} \tag{36}$$

where κ is a very small positive constant showing a boundary layer around zero and can be selected arbitrarily.

In case of $\|\mathbf{s}\| \leq \kappa$, in accordance with Lyapunov criteria and LaSalle extension, it is easily to reveal that $\mathbf{s}$ is guaranteed to be ultimately uniformly bounded in the following compact set

$$\mathbf{U_s} = \left\{\mathbf{s} \in \mathbf{R}^{2\times 1}\,\middle|\,\left(K_{\min} + \frac{\widehat{\Upsilon}}{\kappa}\right)\|\mathbf{s}\| \leq \Upsilon\right\}, \tag{37}$$

where $K_{\min}$ is the minimum eigenvalue of $\mathbf{K}$. Besides, it is worth to note that $\mathbf{s}$ can be kept as small as possible via choosing $\mathbf{K}$ to be suitable. Particularly, the bigger $\mathbf{K}$ is, the smaller $\mathbf{s}$ is.

4. SIMULATION RESULTS

In this section, let us show a computer simulation for trajectory tracking of the WMR which were implemented to validate the correctness and effectiveness of the proposed control method. Crucially, it is unnecessary to preliminary known the dynamic parameters of the WMR precisely. Furthermore, in this computer simulation, we compared between its tracking performance and that of the feedback linearization control method [8].

For comparison, both of the two methods were implemented under the same condition that in addition to the model uncertainties and the bounded external disturbances existing, there was also no need for measuring the accelerations and velocities of the unknown wheel slips. To be specific, without loss generality, let us assume that $\boldsymbol{\tau}_d = [3 + \sin(0.5t), 2.5 + \cos(0.4t)]^T$ (N.m), and furthermore the unknown wheel slips between the floor and the driving wheels are illustrated as $[\dot{\gamma}_R, \dot{\gamma}_L, \dot{\eta}]^T = [2\sin t, 1.5\cos 0.5t, 0.5]^T$ (m/s) for all $t > 2$ (s). The control gains were chosen as $K = \text{diag}([2,2])$, $\boldsymbol{\Lambda} = \text{diag}([2,2])$.

The target D was on a straight line with the following motion equation

$$\begin{cases} x_D = 4 + 0.5t, \\ y_D = -0.5 + 0.25t. \end{cases} \tag{38}$$

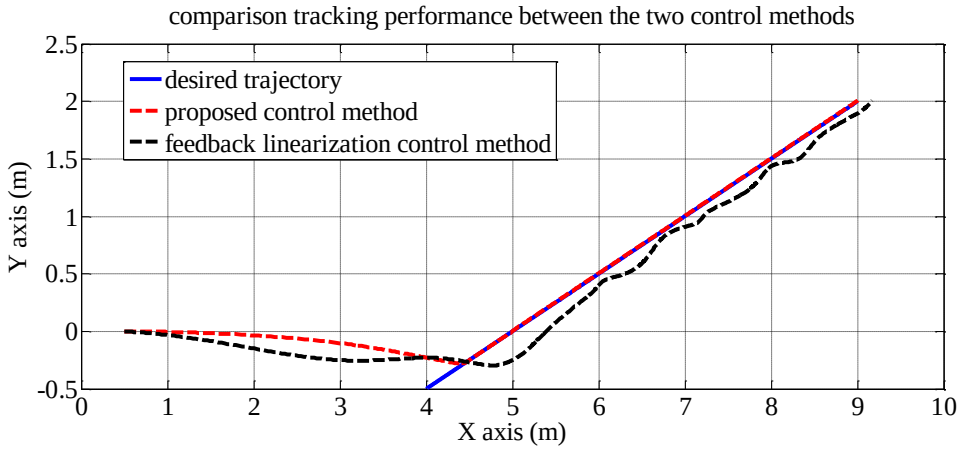

Fig. 3. Comparison of tracking results between two control methods

Simulation results are shown in Fig. 3 and Fig. 4. It is clear from Fig. 3 and Fig. 4 that even though there were no the data of the slip-accelerations and slip-velocities as well as there were the existences of both the model uncertainties and the unknown bounded external disturbances, the proposed control method has effectively compensated the undesired effects of all the wheel slips, model uncertainties, and external disturbances in

comparison with the control method in [8]. In other words, the robust capability of the robust terms gave the former a big advantage over the latter.

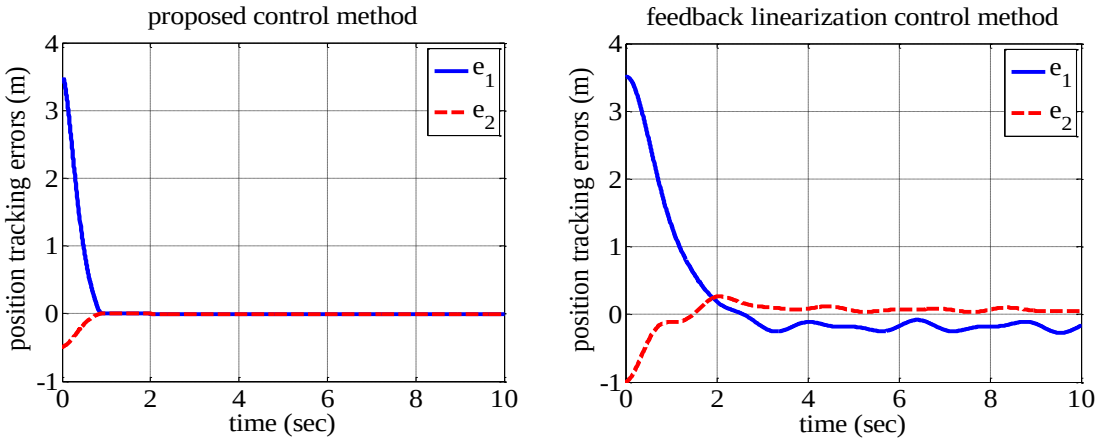

Fig. 4. Comparison of tracking errors between two control methods

It is obvious that the vector of the position tracking errors, **e** in (16), asymptotically converged to zero, and thus also asymptotically converged to the constant C. Therefore, according to Remark 2, it is easy to point out that **h** in (14) is invertible.

It is clear that the vector of the velocity tracking errors, **s**, is asymptotic convergent to zero as shown in Fig. 5. Also, it is clear that the control inputs $\boldsymbol{\omega}$ and the gains of the kinematic and dynamic robust terms, $\widehat{\Gamma}$ and $\widehat{\Upsilon}$, of the proposed control method were bounded as illustrated in Fig. 6.

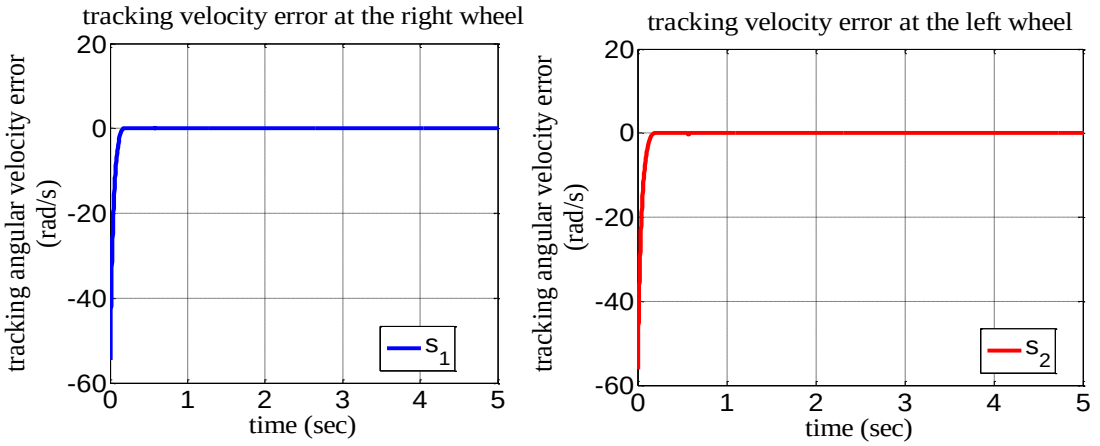

Fig. 5. The evolution of the velocity tracking errors **s**

In general, from these above simulation results, we can draw a conclusion that Theorem 1 holds.

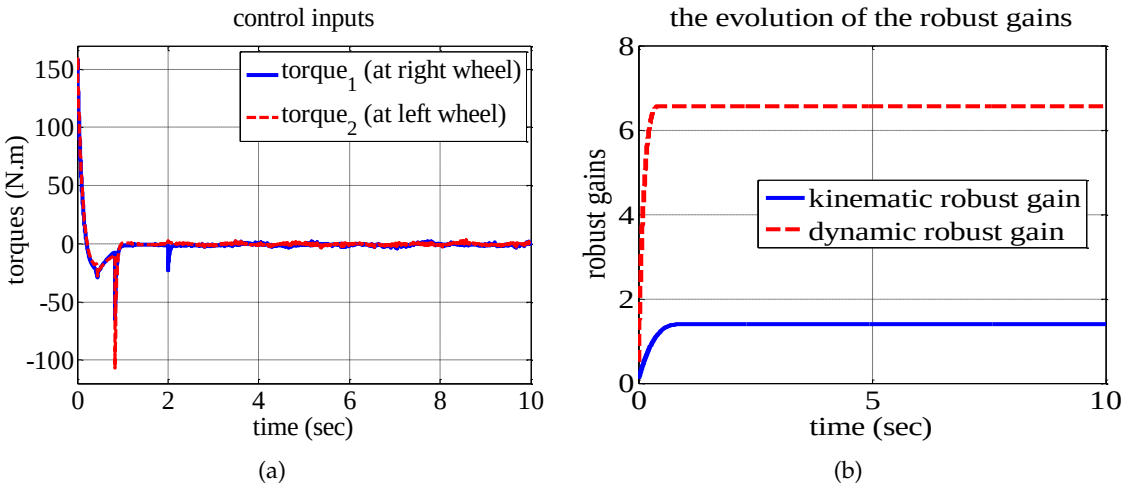

Fig. 6. (a) The evolution of control inputs; (b) The evolutions of the robust gains, $\widehat{\Gamma}$ and $\widehat{Y}$

Remark 5. For the tracking performance of the feedback linearization control method, one may wonder why it is worse in this paper than in the original paper [8]. For comparison purposes, in this paper, both the feedback linearization control method and this proposed control method were simulated under a more realistic condition where apart from ignoring the measurements for the accelerations and velocities of the wheel slips, we have taken into account the existence of both the unknown external disturbances and the model uncertainties. Meanwhile, in the original paper [8], the feedback linearization method was simulated under an ideal condition where the accelerations and velocities of the wheel slips were available from precise measurements, and further there existed no both the external disturbances and the model uncertainties.

5. CONCLUSIONS

In this work, the robust tracking control method has been developed to allow the WMR to track a predefined trajectory with the desired tracking performance in the presence of the unknown wheel slips, model uncertainties, and unknown bounded external disturbances. It is unnecessary to require prior knowledge of the dynamic parameters of the WMR exactly. The two robust terms were utilized to form the robustness of the whole closed-loop control system. Particularly, the one was used in the kinematic controller, and the other was employed in dynamic controller. The gains of the two robust techniques were updated online due to no prior knowledge of the upper bounds of the wheel slips, model uncertainties, and external disturbances. It has been shown that not only the asymptotic convergence of the tracking errors to zero is guaranteed but also the robust terms are bounded via standard Lyapunov theory and LaSalle extension. The results of the computer simulations demonstrated the correctness as well as effectiveness of the proposed control approach.

ACKNOWLEDGMENT

This work is supported by Vietnam Academy of Science and Technology under Grant VAST.01.06/17-18.

REFERENCES

[1] H. M. Becerra, G. López-Nicolás, and C. Sagüés. A sliding-mode-control law for mobile robots based on epipolar visual servoing from three views. *IEEE Transactions on Robotics*, **27**, (1), (2011), pp. 175–183. doi:10.1109/tro.2010.2091750.

[2] B. S. Park, S. J. Yoo, J. B. Park, and Y. H. Choi. A simple adaptive control approach for trajectory tracking of electrically driven nonholonomic mobile robots. *IEEE Transactions on Control Systems Technology*, **18**, (5), (2010), pp. 1199–1206. doi:10.1109/tcst.2009.2034639.

[3] R. Fierro and F. L. Lewis. Control of a nonholonomic mobile robot using neural networks. *IEEE Transactions on Neural Networks*, **9**, (4), (1998), pp. 589–600. doi:10.1109/72.701173.

[4] T. C. Lee, K. T. Song, C. H. Lee, and C. C. Teng. Tracking control of unicycle-modeled mobile robots using a saturation feedback controller. *IEEE Transactions on Control Systems Technology*, **9**, (2), (2001), pp. 305–318. doi:10.1109/87.911382.

[5] H. Gao, X. Song, L. Ding, K. Xia, N. Li, and Z. Deng. Adaptive motion control of wheeled mobile robot with unknown slippage. *International Journal of Control*, **87**, (8), (2014), pp. 1513–1522. doi:10.1080/00207179.2013.878038.

[6] M. Seyr and S. Jakubek. Proprioceptive navigation, slip estimation and slip control for autonomous wheeled mobile robots. In *Proceedings of IEEE Conference on Robotics, Automation and Mechatronics*, Bangkok, (2006). IEEE, pp. 1–6. doi:10.1109/ramech.2006.252627.

[7] C. B. Low and D. Wang. Integrated estimation for wheeled mobile robot posture, velocities, and wheel skidding perturbations. In *Proceedings of IEEE International Conference on Robotics and Automation,*, Roma, (2007). IEEE, pp. 2355–2360. doi:10.1109/robot.2007.363671.

[8] N. V. Tinh, N. T. Linh, P. T. Cat, P. M. Tuan, M. N. Anh, and N. P. Anh. Modeling and feedback linearization control of a nonholonomic wheeled mobile robot with longitudinal, lateral slips. In *Proceedings of IEEE International Conference on Automation Science and Engineering (CASE)*, Fort Worth, (2016). IEEE, pp. 996–1001. doi:10.1109/coase.2016.7743512.

[9] N. B. Hoang and H. J. Kang. Neural network-based adaptive tracking control of mobile robots in the presence of wheel slip and external disturbance force. *Neurocomputing*, **188**, (2016), pp. 12–22. doi:10.1016/j.neucom.2015.02.101.

[10] S. J. Yoo. Approximation-based adaptive control for a class of mobile robots with unknown skidding and slipping. *International Journal of Control, Automation and Systems*, **10**, (4), (2012), pp. 703–710. doi:10.1007/s12555-012-0405-6.

[11] D. Wang and C. B. Low. Modeling and analysis of skidding and slipping in wheeled mobile robots: Control design perspective. *IEEE Transactions on Robotics*, **24**, (3), (2008), pp. 676–687. doi:10.1109/tro.2008.921563.

[12] J. J. E. Slotine and W. Li. *Applied nonlinear control*. Prentice-Hall, (1991).